RESEARCH ARTICLE | DECEMBER 09 2024

Chromatin folding through nonuniform motorization by responsive motor proteins

Special Collection: Chromatin Structure and Dynamics: Recent Advancements

Zhiyu Cao ; Peter G. Wolynes

J. Chem. Phys. 161, 224903 (2024)
https://doi.org/10.1063/5.0238294

The Journal of Chemical Physics ARTICLE pubs.aip.org/aip/jcp

Chromatin folding through nonuniform motorization by responsive motor proteins

Cite as: J. Chem. Phys. 161, 224903 (2024); doi: 10.1063/5.0238294
Submitted: 10 September 2024 • Accepted: 26 November 2024 •
Published Online: 9 December 2024

Zhiyu Cao[1] and Peter G. Wolynes[1,2,3,a)]

AFFILIATIONS

[1] Center for Theoretical Biological Physics, Rice University, Houston, Texas 77005, USA
[2] Department of Chemistry, Rice University, Houston, Texas 77005, USA
[3] Department of Physics, Rice University, Houston, Texas 77005, USA

Note: This paper is part of the JCP Special Topic on Chromatin Structure and Dynamics: Recent Advancements.
[a)]**Author to whom correspondence should be addressed:** pwolynes@rice.edu

ABSTRACT

Chromatin is partially structured through the effects of biological motors. "Swimming motors" such as RNA polymerases and chromatin remodelers are thought to act differentially on the active parts of the genome and the stored inactive part. By systematically expanding the many-body master equation for chromosomes driven by swimming motors, we show that this nonuniform aspect of motorization leads to heterogeneously folded conformations, thereby contributing to chromosome compartmentalization.

I. INTRODUCTION

Chromatin is a complex heteropolymer composed of genomic DNA and associated proteins, regulated by various proteins, some of which are active motors.[1] Advances in imaging and sequencing technologies show this structure is overall disordered but varies in its statistics between active and inactive regions.[2–5] Chromosome Conformation Capture (Hi-C) experiments measure this separation by quantifying contact probabilities within euchromatic (A) and heterochromatic (B) regions and then showing an effective relative repulsion between them.[6] The formation of these "A/B compartments" is often attributed to pairwise attractions between chromatin segments.[7]

Many chromatin-associated proteins may be thought of as motors.[8–10] RNA polymerase II, a swimming motor, clearly acts heterogeneously.[11–13] Other proteins also play an important role in setting up the folding patterns of chromosomes in different cell types and states.[4,14,15] A heterogeneous chromatin folding model based on energy landscape theory trained to maximize the information-theoretical entropy consistent with observed patterns (Minimal Chromatin Model[16] or MiChroM[17–22]) indicates that the compartmentalization of chromosomes can be effectively pictured as coming from the microphase separation of regions with different biochemical properties. In this model, the formation of folding patterns is described as coming from heterogeneous effective static interactions between parts of the chromosome. The detailed biophysical mechanisms are not spelled out in this analysis. Recently, we analyzed the folding patterns of a homogeneous motorized chromosome model, where the response of the motors to imposed forces is critical.[23] Many other models of nonequilibrium motors assume the motors act independently of the forces that they must exert.[24–31]

Here, we explore the statistical mechanical modeling of a heterogeneous chromosome model with force-responsive swimming motors. We do not deal with grappling motors, which we have shown can naturally lead to long-ranged correlations that show up in the "ideal chromosome."[16–19,32,33] In the present model, chromosomes are driven by swimming motors, giving rise to a many-body master equation for their configurations, similar to previous studies on the cytoskeleton[34–37] and on uniform chromosome chains.[23] By systematically expanding the master equation, we show that motor-driven compartments will be separated from the non-motor-driven compartments at their junctions. Analytical and numerical analyses of this minimal model show that the effect of nonuniform motorization induces direct mode coupling and can be mapped as non-local interactions in an equivalent effective equilibrium model.[23,29]

II. MODEL

Here we study a nonuniform, sequence-dependent motorized model of a heteropolymer separated into euchromatin (A) and

heterochromatin (B) regions. Following our previous work,[23] we describe the motion of the motorized chain by an overdamped Langevin equation to which is added discrete steps mimicking the kicks of the motors: $\dot{\mathbf{r}}_i = \beta D(-\nabla_i U) + \boldsymbol{\eta}_i + \mathbf{v}_i^m$, where $\mathbf{r}_i$ is the position of the ith bead of the polymer. We take the backbone to be a Rouse chain, thereby neglecting excluded volumes, so that the potential is harmonic, $U(\{\mathbf{r}\}) = U(\mathbf{r}_1, \mathbf{r}_2, \ldots, \mathbf{r}_n) = K\sum_{i=1}^{N} (\mathbf{r}_i - \mathbf{r}_{i-1})^2/2$ with K the spring constant. The random variables $\boldsymbol{\eta}_i$ are Gaussian noises, representing the ordinary thermal Brownian random forces with zero average correlated in the usual way as $\langle \eta_{i_1}^{j_1}(t)\eta_{i_2}^{j_2}(t')\rangle = 2D\delta_{i_1 i_2}\delta_{j_1 j_2}\delta(t-t')$, where D is the diffusion coefficient and β is the inverse temperature. The kicking terms from the motors $\mathbf{v}_i^m = \sum_q \mathbf{l}_q \delta(t - t_q)$ are modeled as a time series of shot-noise-like transitions. The statistical nature of the motor kicks depends on how the motor's activity is influenced by the applied forces and how far the motor displaces the chain elements in each step. We see that this activity dependence implies the statistics of $\mathbf{v}_i^m$ is *not* independent of chain structure—a crucial difference from some other models of motorized chromosomes and active matter.[24–31,38–40] This description leads to a Master equation to track the dynamics of the probability distribution function Ψ of the chain having bead positions in three-dimensional space $\{\mathbf{r}_i\}$, $\partial_t \Psi_t(\{\mathbf{r}\}) = (\mathcal{L}_{FP} + \mathcal{L}_{NE})\Psi_t(\{\mathbf{r}\})$. The first term $\mathcal{L}_{FP}\Psi_t(\{\mathbf{r}\}) = -\sum_i \nabla_i \cdot \mathbf{J}_i$ is the conventional Fokker–Planck operator describing the passive thermal motions with $\mathbf{J}_i(\{\mathbf{r}\};\ t) = \beta D(-\nabla_i U)\Psi_t(\{\mathbf{r}\}) - D\nabla_i \Psi_t(\{\mathbf{r}\})$ the probability current. The statistics of the nonequilibrium motorized displacements of the chain by the motors are summarized by an integral term in the Master equation $\mathcal{L}_{NE}\Psi_t(\mathbf{r}) = \int \Pi_i d\mathbf{r}_i' K_{\mathbf{r}'\to\mathbf{r}} \Psi_t(\mathbf{r}') - \Psi_t(\mathbf{r}) \int \Pi_i d\mathbf{r}_i' K_{\mathbf{r}\to\mathbf{r}'}$, where $K_{\mathbf{r}'\to\mathbf{r}}$ is the transition rate between different chain conformations caused by a single specific kicking event. The kicking rate depends on how the underlying biochemical mechanisms of the motors respond to the forces that are required to displace them. We write $k = \kappa W(\Delta U) = \kappa[\Theta(\Delta U)e^{-\vartheta_u \beta \Delta U} + \Theta(-\Delta U)e^{-\vartheta_d \beta \Delta U}]$ with κ the basal kicking rate, Θ the Heaviside function, and ΔU the free energy difference between the starting configuration and the displaced chain due to the motorization.[34–37,41,42] This discrete dynamics resembles a typical finite-step Monte–Carlo move. Our setup, we see, couples motor-driven non-equilibrium chemical reactions with the local mechanical forces acting on the motors. The assumption that transition probabilities depend instantaneously on the particle configuration implies that the dynamics is Markovian. Processivity requires additional variables monitoring how long a motor has been actively bound to the chromosome fiber. The coefficient ϑ, called the susceptibility, describes the coupling strength between the kicking noises and mechanical interactions. Susceptibilities have been measured for many systems by using force-extension measurements.[43,44] The motor susceptibilities can be different for uphill kicks (ϑ_u) and downhill kicks (ϑ_d). These coefficients depend on the motor mechanism. When $\vartheta \to 0$, the motors do not respond to external forces. We say here in that case that the motors are "fully adamant." When $\vartheta \neq 0$, the motor responds to applied forces.

In active matter research, it has been common to model motors as transporting their cargo directly across three-dimensional space. True molecular-level swimming typically involves only minute movements.[45] We called motors, which relocate individual elements, "swimming motors" in our previous work.[23] Conceptually, this type of motor can be thought of as approximating the local reorganization of chromatin facilitated by active nuclear enzymes such as RNA polymerase II, helicases, or topoisomerases.[46–49] These proteins act on local chromatin structures to regulate DNA accessibility, structural states, or topological properties, thus forming the basis for dynamic chromatin regulation. RNA polymerase II unwinds the DNA double helix during transcription, transcribing the template strand into mRNA while closely interacting with both DNA and RNA.[50,51] Its size is ~10–12 nm,[52] with a typical transcriptional activity range spanning several kbps to 10 kbps.[53] Helicases primarily function to unwind DNA or RNA duplexes during replication, transcription, or repair, enabling local single-strand formation.[54] Their size ranges from 5 to 15 nm, depending on the specific type,[55] with an activity range typically covering hundreds to thousands of base pairs.[56] Topoisomerases alleviate torsional stress and resolve supercoiling by cutting and rejoining DNA strands, maintaining DNA topology. Their size is ~8–10 nm,[57] and they locally act on DNA segments spanning hundreds to thousands of base pairs to manage supercoils and topological stress.[58]

For simplicity in this paper, we will show results only for the choice $\vartheta_u = \vartheta_d = \vartheta$ but our results are easily generalized to the two susceptibilities being different. Motors with both signs of ϑ are known. We here will mainly focus on motors with nonnegative ϑ. A swimming motor executes a power stroke, leading to a specific structural alteration that propels the polymer bead by a distance l in the direction $\mathbf{n}$, denoted as $\mathbf{l} = l\mathbf{n}(\boldsymbol{r})$. The transition rate kernel $K_{\mathbf{r}'\to\mathbf{r}}$ for swimming motors can then be written as

$$\begin{aligned}\mathcal{L}_{NE}\Psi_t(\mathbf{r}) = \kappa\sum_i \int d\mathbf{n}\Big\{ & e^{-\vartheta\beta[U(\ldots,\mathbf{r}_i,\ldots)-U(\ldots,\mathbf{r}_i-\mathbf{l},\ldots)]} \\ & \times \Psi_t(\ldots,\mathbf{r}_i' = \mathbf{r}_i - \mathbf{l},\ldots) - e^{-\vartheta\beta[U(\ldots,\mathbf{r}_i+\mathbf{l},\ldots)-U(\ldots,\mathbf{r}_i,\ldots)]} \\ & \times \Psi_t(\ldots,\mathbf{r}_i,\ldots)\Big\}. \end{aligned} \tag{1}$$

The basal kicking rate may depend on the conformation of the chromosome chain.[45] Here, we assume that the kicking direction $\mathbf{n}$ fluctuates on the timescale of the motor particle's tumbling $\tau \ll \kappa^{-1}$, which corresponds to an isotropic kicking process. Polymerases swim along the chain, but because of the thermal motions of the chain, they lead to a small persistence length statistically. We believe isotropy then is an appropriate approximation to describe the motions on the larger length scales.

Although previous studies based on MiChroM suggest that static interactions between local chromatin types can predict specific patterns of compartmentalization in the genome,[18] the detailed biophysical mechanisms that give rise to those interactions are not specified. We focus on the case where the sequence-dependent activity of polymerase along the chain is only the monomers in the A (euchromatin) segments that are affected by the swimming motors. Then we have explicitly a uniform thermal motion,

$$\mathcal{L}_{FP}\Psi_t(\mathbf{r}) = -\sum_{i\in A\cup B} \nabla_i \cdot [\beta D(-\nabla_i U)\Psi_t(\mathbf{r}) - D\nabla_i \Psi_t(\mathbf{r})], \tag{2}$$

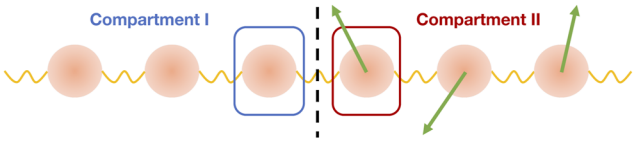

FIG. 1. Model of the genome as a heteropolymer with nonuniform motorization. As a minimal model, we assume uniform activity within segments I and II. Specifically, $\kappa_{i\in I} = 0$ for heterochromatin and $\kappa_{i\in II} = \kappa$ for euchromatin.

and a heterogeneous motorized effect described as

$$\mathcal{L}_{NE}\Psi_t(\mathbf{r}) = \sum_{i\in A}\kappa_i \int d\mathbf{n}\Big\{e^{-\vartheta\beta[U(\ldots,\mathbf{r}_i,\ldots)-U(\ldots,\mathbf{r}_i-\mathbf{l},\ldots)]} \times \Psi_t(\ldots,\mathbf{r}_i'=\mathbf{r}_i-\mathbf{l},\ldots) - e^{-\vartheta\beta[U(\ldots,\mathbf{r}_i+\mathbf{l},\ldots)-U(\ldots,\mathbf{r}_i,\ldots)]} \times \Psi_t(\ldots,\mathbf{r}_i,\ldots)\Big\}. \quad (3)$$

To elucidate how heterogeneous motorizations affect the polymer conformation, we study the simplest case where there are only two continuous segments, one made up of heterochromatin (B compartment) having $\kappa = 0$ and the other having $\kappa_{i\in II} = \kappa$ for the euchromatin or A compartment, see Fig. 1. A junction is placed at the middle of the chain.

III. PÉCLET NUMBER EXPANSION

When the kicks are relatively small, one can expand the nonequilibrium integral operator perturbatively as

$$\mathcal{L}_{NE}\Psi_t(\mathbf{r}) = -\sum_{i\in A}\nabla_i\cdot\left[\frac{\vartheta\kappa_i l^2}{d}(-\nabla_i\beta U)\Psi_t(\mathbf{r}) - \frac{\kappa_i l^2}{2d}\nabla_i\Psi_t(\mathbf{r})\right]. \quad (4)$$

Here, d is the general dimension. Wang and Wolynes showed that in cytoskeleton models, this can be described as a renormalization of the diffusion coefficients and the ambient temperature.[37] Here, the effect of the heterogeneous motorization is to yield a sequence-dependent diffusion constant and sequence-dependent effective temperature of the Brownian motion,

$$\beta_{\text{eff},i\in II} = \beta\left[1+\left(\vartheta-\frac{1}{2}\right)\frac{\Delta}{d}\right], \quad (5)$$

$$D_{\text{eff},i\in II} = D\left(1+\frac{\vartheta\Delta}{d}\right). \quad (6)$$

The non-uniformity of effective temperature leads to spatial structure. The quantity $\Delta = \kappa l^2/D$ is analogous to the Péclet number used in discussing diffusion in systems with convection. In hydrodynamics, the Péclet number quantifies the effects of flows relative to the effects of molecular diffusion.[59]

IV. EFFECTIVE ROUSE MODE ANALYSIS

Without considering the excluded volume effect, we see the renormalized temperature and diffusion coefficient lead to an effective Rouse model to low order in the Péclet number. This is most easily seen in the continuous version of the model appropriate for a long polymer chain composed of a large number of beads: $\mathbf{r}_i(t) \to \mathbf{r}(s,t)$ as $\partial_t\mathbf{r}(s,t) = (\beta D)K\partial_s^2\mathbf{r}(s,t) + \boldsymbol{\eta}(s,t)$, where $\boldsymbol{\eta}(s,t)$ is the Gaussian random noise.[60,61] The Rouse mode decomposition is basically a sequence Fourier transformation, written as follows: $\mathbf{r}(s,t) \to \hat{\mathbf{r}}_q(t) = \int_{-L/2}^{L/2} ds e^{-iqs}\mathbf{r}(s,t)$ and $\boldsymbol{\eta}(s,t) \to \hat{\boldsymbol{\eta}}_q(t) = \int_{-L/2}^{L/2} ds e^{-iqs}\boldsymbol{\eta}(s,t)$, where L is the polymer length. We use two matrices $\hat{\mathbf{R}}_{q,\ldots}(t) = \hat{\mathbf{r}}_q(t)$ and $\hat{\mathbf{M}}_{q,\ldots}(t) = \hat{\boldsymbol{\eta}}_q(t)$ to represent the Rouse modes, where the Rouse mode dynamics can be written as $\partial_t\hat{\mathbf{R}}(t) = -\mathbf{J}(t)\cdot\hat{\mathbf{R}}(t) + \mathbf{H}(t)$. Here, $\mathbf{J}$ is the response matrix and $\mathbf{H}(t)$ is the covariance matrix with $\langle\mathbf{H}(t)\mathbf{H}^\dagger(t')\rangle = \boldsymbol{\Lambda}\delta(t-t')$.[60,61] The spatial association of chromosomal steady-state configurations can be analyzed by calculating the second Rouse moments of the displacements[23,29] $\mathbf{Y} = \lim_{t\to\infty}\langle\hat{\mathbf{R}}(t)\cdot\hat{\mathbf{R}}^\dagger(t)\rangle/L$. In the long time limit, the steady-state solution can be obtained as

$$\mathbf{Y} = L^{-1}\int_0^\infty d\tau e^{-\mathbf{J}\tau}\cdot\boldsymbol{\Lambda}\cdot e^{-\mathbf{J}^\dagger\tau}. \quad (7)$$

For convenience, we apply the periodic boundary condition to the entire chain, which eliminates the need to address end effects. By transforming the second Rouse moments into real space, we can obtain the mean squared separation $\langle\mathbf{r}_{ss'}^2(t)\rangle$ with $\mathbf{r}_{ss'}(t) = \mathbf{r}(s,t) - \mathbf{r}(s',t)$, which characterizes the structural patterns in the polymer conformation.

V. NONUNIFORM HETEROPOLYMER CHAIN WITH COMPARTMENTALIZATION

For the motorized chain whose response matrix is non-diagonal, we assume that the interactions within the backbone Rouse chain (the diagonal elements of the response matrix) are dominant. The other interactions caused by the motors are perturbations ($\delta J_{qk,q\neq k} \ll J_{qk,q=k}$), and the covariance matrix between different modes can be decomposed into the independent parts with homogeneous magnitude Λ_0 and the correlated parts $\Lambda_{qk,q\neq k}$. Following the method proposed by Goychuk *et al.*,[29] we calculate the second Rouse moments by using the matrix exponential perturbation as $LY_{qk} = \frac{\Lambda_{qk}}{J_{qq}+J_{kk}} - \frac{\Lambda_0}{J_{qq}+J_{kk}}\left(\frac{\delta J_{qk}}{J_{kk}} + \frac{\delta J_{kq}^*}{J_{qq}}\right)$.[62] For the minimal scenario studied here, we place the II compartment (euchromatin) on the right-hand segment $s\in(0,L/2]$, which is subject to swimming motors, and the I compartment (heterochromatin) on the left-hand segment $s\in[-L/2,0]$, which is not subjected to swimming motors. Thus, we take

$$\kappa(s) = \begin{cases} 0 & s\in[-L/2,0] \\ \kappa & s\in(0,L/2] \end{cases}, \quad (8)$$

where the junction between the two compartments, one active and the other inactive, is placed at $s = 0$. From Eqs. (5) and (6), the effects of motorization lead to sequence-dependent effective diffusion $D_{\text{eff}}(s)$ and effective temperature $\beta_{\text{eff}}(s)$,

$$D_{\text{eff}}(s) = \begin{cases} D & s\in[-L/2,0] \\ D\left(1+\frac{\Delta}{2d}\right) & s\in(0,L/2] \end{cases}, \quad (9)$$

and

$$\beta_{\text{eff}}(s) = \begin{cases} \beta & s \in [-L/2, 0] \\ \beta\left[1 + \left(\vartheta - \frac{1}{2}\right)\frac{\Delta}{d}\right] & s \in (0, L/2] \end{cases}. \quad (10)$$

From that we obtain

$$Y_{qk} = \frac{b^2\delta_{qk}}{q^2} - \frac{2b^2 f_{q-k}}{L(q^2+k^2)}. \quad (11)$$

Here, f_q is the sequence Fourier transformation of $f(s)$ with $f(s) = 0$ for $s \in [-L/2, 0]$ and $f(s) = (\vartheta - \frac{1}{2})\Delta/d$ for $s \in (0, L/2]$. It is worth noting that, unlike a homogeneous chain, a heterogeneous chain with nonuniform motorization couples different Rouse modes having different sequence k vectors. By transforming Eq. (11) back into real sequence space, we obtain the spatial correlations of the chromosome with heterogeneous motorization,

$$\langle \mathbf{r}(s,t) \cdot \mathbf{r}(s',t) \rangle = -\frac{1}{2}b^2\left[|\Delta s| - \int dx f(x) G^A(s-x, s'-x)\right], \quad (12)$$

where $\Delta s = s - s'$ and $G^A(s_1, s_2) = [2\gamma_e + \log(s_1^2 + s_2^2)]/\pi$ is the Green's kernel with γ_e, the Euler–Mascheroni constant.

By using Eq. (12), one can analytically calculate the mean squared separation $\langle \mathbf{r}_{ss'}^2(t) \rangle$ for the heterogeneous polymer chains subjected to swimming motors with different susceptibilities, see Fig. 2(a). Where the susceptible motors drive the polymer chain, the mean squared separations become smaller; whereas, if the chain is driven by adamant motors, the mean squared separations become larger. To illustrate this more clearly, we present the changes in mean squared separation relative to a passive Rouse polymer in Fig. 2(b). The junction breaks the sequence translational invariance. When the system is driven by susceptible motors, the active regions not only contract themselves significantly but also cause a slight contraction in those parts of the inactive region near the junction. Conversely, when driven by adamant motors, the active regions expand significantly but at the same time also cause a slight expansion in the inactive regions close to the junction. This suggests that the driving forces of motors with different properties may contribute to compartmentalization locally in sequence but only throughout three dimensions.

VI. NONUNIFORM MOTORIZATIONS INDUCED LONG-RANGED INTERACTIONS

To elucidate the conformation of motorized chains, we note that any Gaussian steady state can be mapped to the thermal equilibrium weight of a generalized Gaussian polymer with additional harmonic interactions,[23,29,63] where the dynamics of the polymer are determined by

$$\begin{aligned} \partial_t \mathbf{r}(s,t) &= \beta D k\left\{\partial_s^2 \mathbf{r}(s,t) + \int ds' \tilde{\mathcal{K}}(s,s')[\mathbf{r}(s',t) - \mathbf{r}(s,t)]\right\} + \eta(s,t) \\ &= \beta D k\Big\{\partial_s[(1 + \tilde{\mathcal{K}}(s))\partial_s \mathbf{r}(s,t)] \\ &\quad + \int ds' \tilde{\mathcal{K}}_{LR}(s,s')[\mathbf{r}(s',t) - \mathbf{r}(s,t)]\Big\} + \eta(s,t). \end{aligned} \quad (13)$$

In the second equality, the additional interactions caused by the motorizations decouple into a local reorganization term $\tilde{\mathcal{K}}(s)$ and a direct interaction term $\tilde{\mathcal{K}}_{LR}(s,s')$ with reciprocity that is $\tilde{\mathcal{K}}_{LR}(s,s') = \tilde{\mathcal{K}}_{LR}(s',s)$, which can be positive or negative. We can extract the coupling coefficients $\tilde{\mathcal{K}}(s,s')$ that best reproduce the steady-state separations. To this goal, we first calculate the response matrix of the polymer, which is given by a non-diagonal Hermitian matrix $J_{qk} = \xi^{-1}k(q^2\delta_{qk} - L^{-1}\tilde{\mathcal{K}}_{qk})$. Then, we can obtain that $Y_{qk} = b^2\delta_{qk}/q^2 + b^2\tilde{\mathcal{K}}_{qk}/Lq^2k^2$. Compared with Eq. (11), we can extract the coupling strength to map the motorized chain conformation:

$$\frac{\tilde{\mathcal{K}}_{qk}}{q^2k^2} = -\frac{2f_{q-k}}{q^2+k^2}. \quad (14)$$

Transforming Eq. (14) into real space, one finds that

$$\tilde{\mathcal{K}}(s) = f(s), \quad (15)$$

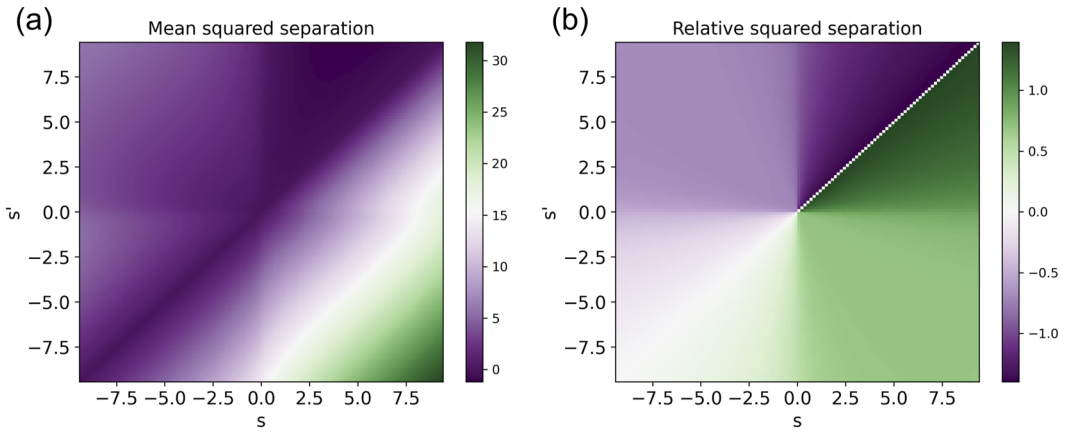

FIG. 2. The mean-squared separation (a, left panel) and change in mean squared separation relative to passive Rouse polymers (b, right panel) of motorized polymer chains for both the susceptible swimming motor ($\vartheta = 1$, upper triangle) and the adamant swimming motor ($\vartheta = 0$, bottom triangle). The results were obtained by numerically calculating Eq. (12). Parameters $L = 8\pi$, $\kappa l^2/dD = 0.6$, and $b^2 = 1$ for both panels.

and

$$\tilde{\mathcal{K}}_{LR}(s,s') = -\int \frac{dq}{2\pi} f_q \frac{|q|^3}{4} e^{-\frac{|q||s-s'|}{2} + \frac{iq(s+s')}{2}}. \tag{16}$$

The first term, Eq. (15), represents the modification of the local spring constant, which renormalizes the effective Kuhn lengths. The second term, Eq. (16), represents the non-local long-range interactions, which give rise to correlations.

As an example, for the minimal model with compartmentalization that we introduced before [see Eq. (8)], we have

$$\tilde{\mathcal{K}}(s) = \begin{cases} 0 & s \in [-L/2, 0] \\ \left(\vartheta - \frac{1}{2}\right)\frac{\Delta}{d} & s \in (0, L/2] \end{cases}, \tag{17}$$

and

$$\tilde{\mathcal{K}}_{LR}(s,s') = -2\left(\vartheta - \frac{1}{2}\right)\frac{\Delta}{d}\int_0^L \frac{dq}{2\pi}\frac{q^2}{4} e^{-\frac{q}{2}|s-s'|} \times \left[\sin\frac{(s+s')}{2}q - \sin\frac{(s+s'-L)}{2}q\right]. \tag{18}$$

For the local modification term, Eq. (17), we observe that the local spring constants of the compartments driven by motors are renormalized, whereas those of the compartments not driven by motors remain unchanged. If the motors are susceptible, the Kuhn length of the motorized compartment will decrease, whereas if the motors are adamant, the Kuhn length of the motorized compartment will increase. This is consistent with our previous findings on uniform motorized chromosomes, where again susceptible motors cause local contraction of the chain, while adamant motors cause local expansion.[23]

We numerically calculate the long-ranged interaction term $\tilde{\mathcal{K}}_{LR}(s,s')$ by using Eq. (18). The results are shown in Fig. 3. We observe that nonuniform motorization yields differently correlated domains near the junction. In some regions, sites exhibit mutual attraction, while in other regions, sites exhibit mutual repulsion. These regions are interleaved along both sides of the junction, with their arrangement dependent on the mechanical properties of the motors. When the motors are susceptible, the regions near the junction driven by the motors show mutual attraction between sites, leading to compaction. Conversely, when the motors are adamant, the regions near the junction show mutual repulsion between sites, leading to expansion.

To see it more clearly, we plot the nonuniform motor-induced long-ranged interactions $\tilde{\mathcal{K}}_{LR}(s,s')$ at different values $\bar{s} = (s+s')/2$ as a function of $\Delta s = s - s'$ for both the adamant motor and the susceptible motor in Fig. 4(a). In Fig. 4(b), we also plot $\tilde{\mathcal{K}}_{LR}(s,s')$ vs $\Delta s = s - s'$ for fixed $s' = 0$, which is close to the junction. Regardless of whether the motors are susceptible or adamant, the motorization-induced interactions between compartments I and II are small. In addition, it is observed that the strength of the motorization-induced interactions decays with increasing distance from the junction. Our calculations indicate that the range of this long-range interaction spans approximately several hundred kilobases. Specifically, for human chromosomes, this length scale is not too different from the typical size of Topologically Associating Domains (TADs), which generally range between 100 kb and 1 Mb.[64] In contrast, compartmentalization often involves larger chromatin structures on the scale of several megabases or even entire chromosomes.[6,65] We suggest that to explain the larger size compartmentalization by swimming motors alone may require multi-junction cooperation. We suggest using this interaction pattern near the junctions of Hi-C data. This junction effect is absent in the very powerful MiChroM model of chromosome structure.[17–22] A careful inspection of directly inverted Hi-C data near such junctions may provide a route to quantify the importance of swimming motors in determining chromosome structure.

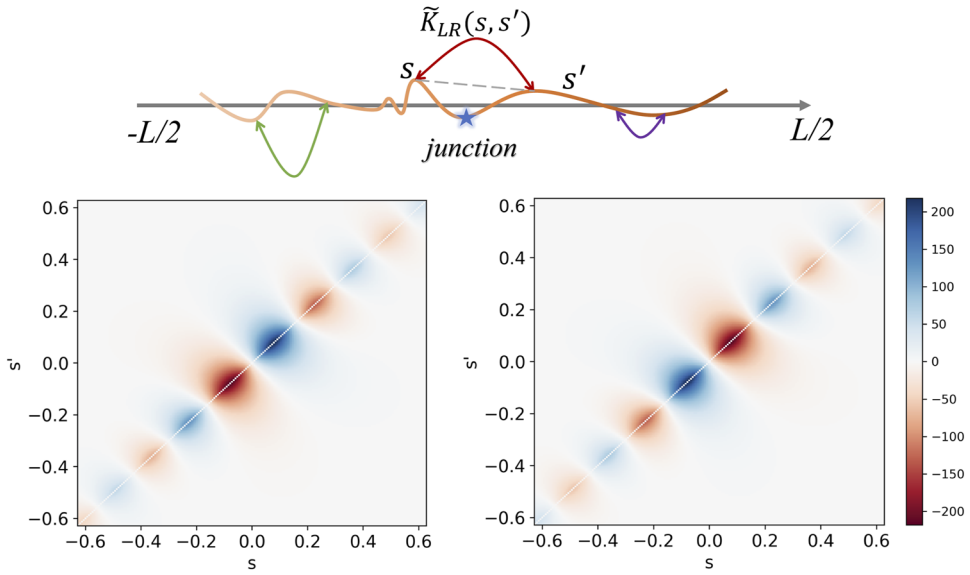

FIG. 3. The nonuniform motorization induced long-ranged interactions $\tilde{\mathcal{K}}_{LR}(s,s')$ for both the adamant swimming motor ($\vartheta = 0$, left panel) and the susceptible swimming motor ($\vartheta = 1$, right panel). The results were obtained by numerically calculating Eq. (18). Parameters: $L = 8\pi$, $\kappa l^2/dD = 0.6$, and $b^2 = 1$.

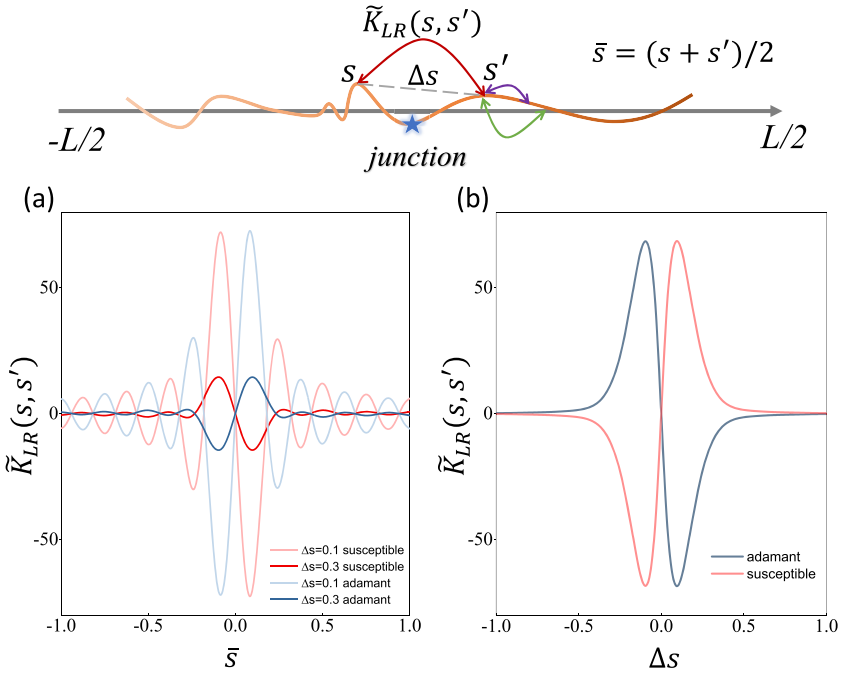

FIG. 4. The nonuniform motorization induced long-ranged interactions $\tilde{K}_{LR}(s,s')$ for both the adamant swimming motor and the susceptible swimming motor. (a) $\tilde{K}_{LR}(s,s')$ are plotted vs $\bar{s}=(s+s')/2$ by varying the genomic separation Δs. (b) $\tilde{K}_{LR}(s,s')$ are plotted vs $\Delta s = s - s'$ for fixed $s' = 0$, near the junction. Parameters: $L = 8\pi$, $\kappa l^2/dD = 0.6$, and $b^2 = 1$.

VII. CONCLUSION

In this paper, we have studied the heterogeneous folding patterns induced by nonuniform motorization. An interaction structure emerges in the junctions between active and inactive components. One can test whether heterogeneous activity profiles of motors with different properties match orthogonal experimental measurements, such as DNA-binding patterns of active enzymes.[66] In addition, a topic worth further investigation is how the combined actions of swimming motors and other "grappling" motors, such as the SMC complex, conspire to organize chromosome conformation. This is left for future work.

ACKNOWLEDGMENTS

This work was supported by both the Bullard–Welch Chair at Rice University, Grant No. C-0016, and the Center for Theoretical Biological Physics sponsored by NSF Grant No. PHY-2019745.

AUTHOR DECLARATIONS

Conflict of Interest

The authors have no conflicts to disclose.

Author Contributions

Zhiyu Cao: Conceptualization (equal); Formal analysis (equal); Methodology (equal); Writing – original draft (equal); Writing – review & editing (equal). **Peter G. Wolynes**: Conceptualization (equal); Formal analysis (equal); Funding acquisition (equal); Methodology (equal); Writing – original draft (equal); Writing – review & editing (equal).

DATA AVAILABILITY

The data that support the findings of this study are available from the corresponding author upon reasonable request.

REFERENCES

[1] T. Misteli, Cell **183**, 28 (2020).
[2] C. P. Brangwynne, P. Tompa, and R. V. Pappu, Nat. Phys. **11**, 899 (2015).
[3] S. F. Banani, A. M. Rice, W. B. Peeples, Y. Lin, S. Jain, R. Parker, and M. K. Rosen, Cell **166**, 651 (2016).
[4] D. Hnisz, K. Shrinivas, R. A. Young, A. K. Chakraborty, and P. A. Sharp, Cell **169**, 13 (2017).
[5] Y. Shin and C. P. Brangwynne, Science **357**, eaaf4382 (2017).
[6] E. Lieberman-Aiden, N. L. Van Berkum, L. Williams, M. Imakaev, T. Ragoczy, A. Telling, I. Amit, B. R. Lajoie, P. J. Sabo, M. O. Dorschner *et al.*, Science **326**, 289 (2009).
[7] M. Falk, Y. Feodorova, N. Naumova, M. Imakaev, B. R. Lajoie, H. Leonhardt, B. Joffe, J. Dekker, G. Fudenberg, I. Solovei, and L. A. Mirny, Nature **570**, 395 (2019).
[8] G. J. Narlikar, R. Sundaramoorthy, and T. Owen-Hughes, Cell **154**, 490 (2013).
[9] F. Uhlmann, Nat. Rev. Mol. Cell Biol. **17**, 399 (2016).
[10] M. A. Reid, Z. Dai, and J. W. Locasale, Nat. Cell Biol. **19**, 1298 (2017).
[11] K. Rippe, Cold Spring Harbor Perspect. Biol. **14**, a040683 (2022).
[12] H. Salari, G. Fourel, and D. Jost, Nat. Commun. **15**, 5393 (2024).
[13] O. Adame-Arana, G. Bajpai, D. Lorber, T. Volk, and S. Safran, eLife **12**, e82983 (2023).
[14] S. Shin, G. Shi, H. Cho, and D. Thirumalai, Proc. Natl. Acad. Sci. U. S. A. **121**, e2307309121 (2024).
[15] M. Magaña-Acosta and V. Valadez-Graham, Front. Genet. **11**, 600615 (2020).

[16]B. Zhang and P. G. Wolynes, Proc. Natl. Acad. Sci. U. S. A. **112**, 6062 (2015).
[17]M. Di Pierro, B. Zhang, E. L. Aiden, P. G. Wolynes, and J. N. Onuchic, Proc. Natl. Acad. Sci. U. S. A. **113**, 12168 (2016).
[18]M. Di Pierro, R. R. Cheng, E. Lieberman Aiden, P. G. Wolynes, and J. N. Onuchic, Proc. Natl. Acad. Sci. U. S. A. **114**, 12126 (2017).
[19]M. Di Pierro, D. A. Potoyan, P. G. Wolynes, and J. N. Onuchic, Proc. Natl. Acad. Sci. U. S. A. **115**, 7753 (2018).
[20]A. B. Oliveira Junior, V. G. Contessoto, M. F. Mello, and J. N. Onuchic, J. Mol. Biol. **433**, 166700 (2021).
[21]V. G. Contessoto, R. R. Cheng, A. Hajitaheri, E. Dodero-Rojas, M. F. Mello, E. Lieberman-Aiden, P. G. Wolynes, M. Di Pierro, and J. N. Onuchic, Nucleic Acids Res. **49**, D172 (2021).
[22]V. G. Contessoto, O. Dudchenko, E. L. Aiden, P. G. Wolynes, J. N. Onuchic, and M. Di Pierro, Nat. Commun. **14**, 326 (2023).
[23]Z. Cao and P. G. Wolynes, Proc. Natl. Acad. Sci. U. S. A. **121**, e2407077121 (2024).
[24]S. C. Weber, A. J. Spakowitz, and J. A. Theriot, Proc. Natl. Acad. Sci. U. S. A. **109**, 7338 (2012).
[25]N. Ganai, S. Sengupta, and G. I. Menon, Nucleic Acids Res. **42**, 4145 (2014).
[26]A. Agrawal, N. Ganai, S. Sengupta, and G. I. Menon, Biophys. J. **118**, 2229 (2020).
[27]Z. Jiang, Y. Qi, K. Kamat, and B. Zhang, J. Phys. Chem. B **126**, 5619 (2022).
[28]A. Ghosh and A. J. Spakowitz, Soft Matter **18**, 6629 (2022).
[29]A. Goychuk, D. Kannan, A. K. Chakraborty, and M. Kardar, Proc. Natl. Acad. Sci. U. S. A. **120**, e2221726120 (2023).
[30]S. Brahmachari, T. Markovich, F. C. MacKintosh, and J. N. Onuchic, PRX Life **2**, 033003 (2024).
[31]A. Goychuk, D. Kannan, and M. Kardar, Phys. Rev. Lett. **133**, 078101 (2024).
[32]B. Zhang and P. G. Wolynes, Phys. Rev. Lett. **116**, 248101 (2016).
[33]B. Zhang and P. G. Wolynes, Biophys. J. **112**, 427 (2017).
[34]T. Shen and P. G. Wolynes, Proc. Natl. Acad. Sci. U. S. A. **101**, 8547 (2004).
[35]T. Shen and P. G. Wolynes, Phys. Rev. E **72**, 041927 (2005).
[36]S. Wang and P. G. Wolynes, Proc. Natl. Acad. Sci. U. S. A. **108**, 15184 (2011).
[37]S. Wang and P. G. Wolynes, J. Chem. Phys. **135** (2011).
[38]C. Bechinger, R. Di Leonardo, H. Löwen, C. Reichhardt, G. Volpe, and G. Volpe, Rev. Mod. Phys. **88**, 045006 (2016).
[39]M. R. Shaebani, A. Wysocki, R. G. Winkler, G. Gompper, and H. Rieger, Nat. Rev. Phys. **2**, 181 (2020).
[40]Z. Cao, H. Jiang, and Z. Hou, J. Chem. Phys. **155** (2021).
[41]S. Wang and P. G. Wolynes, Proc. Natl. Acad. Sci. U. S. A. **109**, 6446 (2012).
[42]S. Wang and P. G. Wolynes, J. Chem. Phys. **136** (2012).
[43]M. Dogterom and B. Yurke, Science **278**, 856 (1997).
[44]J. Howard and R. Clark, Appl. Mech. Rev. **55**, B39 (2002).
[45]X. Bai and P. G. Wolynes, J. Chem. Phys. **143** (2015).
[46]A. B. Kolomeisky and M. E. Fisher, Annu. Rev. Phys. Chem. **58**, 675 (2007).
[47]A. B. Kolomeisky, *Motor Proteins and Molecular Motors* (CRC Press, 2015).
[48]A. Zidovska, D. A. Weitz, and T. J. Mitchison, Proc. Natl. Acad. Sci. U. S. A. **110**, 15555 (2013).
[49]L. Zhang, D.-A. Silva, F. Pardo-Avila, D. Wang, and X. Huang, PLoS Comput. Biol. **11**, e1004354 (2015).
[50]R. D. Kornberg, Proc. Natl. Acad. Sci. U. S. A. **104**, 12955 (2007).
[51]P. Cramer, D. A. Bushnell, J. Fu, A. L. Gnatt, B. Maier-Davis, N. E. Thompson, R. R. Burgess, A. M. Edwards, P. R. David, and R. D. Kornberg, Science **288**, 640 (2000).
[52]K. D. Westover, D. A. Bushnell, and R. D. Kornberg, Science **303**, 1014 (2004).
[53]P. Kapranov, J. Cheng, S. Dike, D. A. Nix, R. Duttagupta, A. T. Willingham, P. F. Stadler, J. Hertel, J. Hackermüller, I. L. Hofacker *et al.*, Science **316**, 1484 (2007).
[54]M. R. Singleton, M. S. Dillingham, and D. B. Wigley, Annu. Rev. Biochem. **76**, 23 (2007).
[55]E. J. Enemark and L. Joshua-Tor, Curr. Opin. Struct. Biol. **18**, 243 (2008).
[56]A. M. Pyle, Annu. Rev. Biophys. **37**, 317 (2008).
[57]J. Roca, Trends Biochem. Sci. **20**, 156 (1995).
[58]J. C. Wang, Nat. Rev. Mol. Cell Biol. **3**, 430 (2002).
[59]P. K. Kundu, I. M. Cohen, and D. R. Dowling, *Fluid Mechanics* (Academic Press, 2015).
[60]M. Doi, S. F. Edwards, and S. F. Edwards, *The Theory of Polymer Dynamics* (Oxford University Press, 1988), Vol. 73.
[61]P.-G. De Gennes, Phys. Phys. Fiz. **3**, 37 (1967).
[62]K. Kumar, J. Math. Phys. **6**, 1928 (1965).
[63]G. Le Treut, F. Képès, and H. Orland, Biophys. J. **115**, 2286 (2018).
[64]J. R. Dixon, S. Selvaraj, F. Yue, A. Kim, Y. Li, Y. Shen, M. Hu, J. S. Liu, and B. Ren, Nature **485**, 376 (2012).
[65]S. S. Rao, M. H. Huntley, N. C. Durand, E. K. Stamenova, I. D. Bochkov, J. T. Robinson, A. L. Sanborn, I. Machol, A. D. Omer, E. S. Lander, and E. Aiden, Cell **159**, 1665 (2014).
[66]K.-S. Leung, K.-C. Wong, T.-M. Chan, M.-H. Wong, K.-H. Lee, C.-K. Lau, and S. K. Tsui, Nucleic Acids Res. **38**, 6324 (2010).